Milling Force Coefficients-based Tool Wear Monitoring for Variable Parameters Milling

Tianhang Pan (pandeng1989@hotmail.com)
Xi'an Jiaotong University
Jun Zhang
Xi'an Jiaotong University
Xing Zhang
Xi'an Jiaotong University
Wanhua Zhao
Xi'an Jiaotong University
Huijie Zhang
Xi'an Jiaotong University
Bingheng Lu
Xi'an Jiaotong University

Research Article

Keywords: Tool wear monitoring, Feature fusion, Milling force coefficients, c-SVM

Posted Date: September 13th, 2021

DOI: https://doi.org/10.21203/rs.3.rs-887538/v1

Version of Record: A version of this preprint was published at The International Journal of Advanced Manufacturing Technology on March 18th, 2022. See the published version at https://doi.org/10.1007/s00170-022-08823-y.

Milling force coefficients-based tool wear monitoring for variable parameters milling

Tianhang Pan, Jun Zhang, Xing Zhang, Wanhua Zhao*, Huijie Zhang, Bingheng Lu

Corresponding author:
Wanhua Zhao
Tel: +86-29-83399520
Fax: +86-29-93399113
E-mail: whzhao@mail.xjtu.edu.cn

Affiliation:
State Key Laboratory for Manufacturing Systems Engineering, Xi'an Jiaotong University, 710054 Xi'an, Shaanxi, China
Address: Room A315 West Building 5, 99# Yanxiang Road, Yanta District, Xi'an, ShaanXi, 710054, China

The affiliations of the co-authors:
State Key Laboratory for Manufacturing Systems Engineering, Xi'an Jiaotong University, 710054 Xi'an, Shaanxi, China

The addresses of the co-authors:
West Building 5, 99# Yanxiang Road, Yanta District, Xi'an, ShaanXi, 710054, China

Milling force coefficients-based tool wear monitoring for variable parameters milling

0. Abstract

Tool wear is an important factor that affects the aeronautical structural parts' quality and machining accuracy in the milling process. It is essential to monitor the tool wear in titanium alloy machining. The traditional tool wear features such as root mean square (RMS), kurtosis, and wavelet packet energy spectrum are related to not only the tool wear status but also to the milling parameters, thus monitoring the tool wear status only under fixed milling parameters. This paper proposes a new method of online monitoring of tool wear using milling force coefficients. The instantaneous cutting force model is used to extract the milling force coefficients which are independent of milling parameters. The principal component analysis (PCA) algorithm is used to fuse the milling force coefficients. Furthermore, support vector machine (SVM) model is used to monitor tool wear states. Experiments with different machining parameters were conducted to verify the effectiveness of this method used for tool wear monitoring. The results show that compared to traditional features, the milling force coefficients are not dependent on the milling parameters, and using milling force coefficients can effectively monitor the transition point of cutters from normal wear to severe wear (tool failure).

Keywords: Tool wear monitoring, Feature fusion, Milling force coefficients, c-SVM

1. Introduction

Due to the lack of manual intervention in an unattended machining system, the tool wear state cannot be judged in the milling process. [1, 2]. Therefore, tool wear monitoring plays an important role in ensuring the quality of the aeronautical structural parts and improving the processing efficiency [3]. In order to maintain good

performance of the cutters, components, and even the machine tools, changing the cutting tool frequently during the milling process must be done, which will affect the efficiency and machining cost. On the other hand, the severe wear tool is not changed timely, the parts even the machine tool will be damaged. Therefore, it is essential to monitor tool wear during the machining process of the aeronautical structural parts.

Many direct and indirect methods have been developed to monitor tool wear. Visual and optical methods are the most direct. D'Addona et al. [4] stops machining after a fixed cutting time and uses a digital camera to photograph the tool wear area. Although this method can accurately judge the condition of tool wear, the measurement process needs to interrupt the machining process, which affects the machining efficiency. Elgargni et al. [5] uses infrared rays and cameras to track and locate the tool in the process of machining, and then judge the tool wear status (normal or damaged). However, because of the continuous contact between the tool and the workpiece and the harsh machining environment (cutting fluid and chip), this method cannot be applied during the actual machining process.

The indirect method makes up for the shortage of direct measurement, which is realized by sensor signals related to tool wear. The tool condition is estimated according to measurable signals, such as forces [6-9], acoustic emission (AE) [10-13], vibration [14-16], and motor current [17-19]. Li [7] extracted 14 time-domain features from forces and established the relationship between time-domain features and tool wear state with the v-SVR model, which was used to monitor the tool wear in turning. Kannatey-Asibu et al. [11] successfully used the AE signal to monitor tool wear using the adaptive classifier learning model. Zhu et al. [20] points out that the AE signal is mostly used to determine tool breakage in the turning process, since the AE signal can reflect the impact characteristics when tool breakage occurs. However, since milling is intermittent, the continuous impact will affect the acoustic emission signal. Khajavi et al. [17] analyzed the influence on the motor content of feed rate, cutting depth, and other parameters on the motor current, and used the multilayer perceptron (MLP) neural network method to predict the tool wear in face milling. A series of experiments were carried out to verify the above method by Khajavi. However, Kim et al. [21] points out

that the milling force will affect the friction of the spindle system/feed system, and then affect the spindle/feed motor current. In order to avoid the single signal cannot accurately determine the tool state, multi-sensorial signals fusion method is used for tool state monitoring [22-31]. Caggiano [22] extracts the time/frequency domain features from the signal of AE, cutting forces, and acceleration then reduces the dimension of the features using the principal component analysis (PCA) method to monitor the tool wear in turning. Stavropoulos et al. [26] combined the vibration in the workpiece and spindle motor current to monitor tool wear during the turning process. Although the method of multi-sensorial signals fusion makes up for the shortcoming of single signals, it needs to have a robust ability of generalization and nonlinear fitting model such as the artificial intelligence model to feature fusion and tool wear monitoring. The artificial intelligence models achieved good results in these research projects, in the application of neural networks [17,27,28], support vector machines [7,29,30], and Markov [31]. However, the above referenced research focus on fixed milling parameters, and few scholars study the monitoring of tool wear under the condition of variable milling parameters.

The essential reason is that the traditional features are not only related to the tool wear but also sensitive to the milling parameters. Therefore, the traditional features are not feasible to monitor tool wear under variable milling parameters during the whole process. In actual machining of the aeronautical structural parts, the milling parameters (feed rate, cutting width, etc.) will change frequently and the machining path is complex. Therefore, it is essential to extract features independent of milling parameters and only related to tool status. The radial and normal cutting force coefficients which are not sensitive to milling parameters are extracted in literature [32]. However, the axial milling force coefficient cannot be ignored. In addition, the threshold can be set when the tool in a state of severe wear, and there are limitations in the practical application of tool wear monitoring.

Aiming at the disadvantage that the traditional feature is obviously affected by milling parameters, the milling force coefficients which are not sensitive to the milling parameters are extracted through the instantaneous milling force model. And the PCA

is then used to fuse the milling force coefficients, and the feature which can reflect the condition of the tool state more clearly is obtained. In addition, with respect to the problem of the threshold setting limited for tool failure, the c-SVM model is used to establish the mapped relationship between the fused features and the actual state of the tool. Tool wear status can be monitored during the process of machining. Finally, experiments with different milling parameters are carried out to verify the proposed method for tool wear status monitoring.

2. Tool wear monitoring based on instantaneous milling force model

2.1 The instantaneous milling force model in flank milling

According to the model of instantaneous rigid force [33], as shown in Fig. 1, the tangential, radial, and axial milling forces of the *j-th* tooth on d*z* can be expressed as:

$$\begin{aligned} \mathrm{d}F_{\mathrm{t}j} &= (K_{\mathrm{tc}} \cdot h(\phi_j) + K_{\mathrm{te}}) \cdot \mathrm{d}z \\ \mathrm{d}F_{\mathrm{r}j} &= (K_{\mathrm{rc}} \cdot h(\phi_j) + K_{\mathrm{re}}) \cdot \mathrm{d}z \\ \mathrm{d}F_{\mathrm{a}j} &= (K_{\mathrm{ac}} \cdot h(\phi_j) + K_{\mathrm{ae}}) \cdot \mathrm{d}z \end{aligned} \tag{1}$$

where K_{qc} and $K_{\mathrm{qe}}(\mathrm{q} = \mathrm{t}, \mathrm{r}, \mathrm{a})$ are the cutting and edge coefficients in the tangential, radial, and axial directions, respectively. $h(\phi_j)$ is the chip thickness, given by

$$h(\phi_j) = f_t \cdot \sin(\phi_j) \tag{2}$$

where f_t is the feed per tooth. $\phi_j = \omega \cdot \mathrm{t} + (j\text{-}1)\phi_p$ is the angle of tooth engagement, ω (rad/s) is the angular velocity of spindle, and $\phi_p = 2\pi / N$ is the inter tooth angle. N is the number of teeth on the cutting tool. By substituting Eq.(2) into Eq.(1), the instantaneous milling force in the coordinate of t, r, and a can be obtained by processing elemental forces of each layer along the *z*-axis of each tooth. Then the forces in the x, y, and z coordinate directions can be expressed as Eq.(3):

$$\begin{bmatrix} F_x(t) \\ F_y(t) \\ F_z(t) \end{bmatrix} = \sum_{j=1}^{N} \int_0^z \mathbf{T} \cdot \begin{bmatrix} dF_{tj}(t) \\ dF_{rj}(t) \\ dF_{aj}(t) \end{bmatrix} \tag{3}$$

where $\mathbf{T}=\begin{bmatrix} -\cos\phi_{jl} & -\sin\phi_{jl} & 0 \\ \sin\phi_{jl} & -\cos\phi_{jl} & 0 \\ 0 & 0 & 1 \end{bmatrix}$ is the transformation matrix.

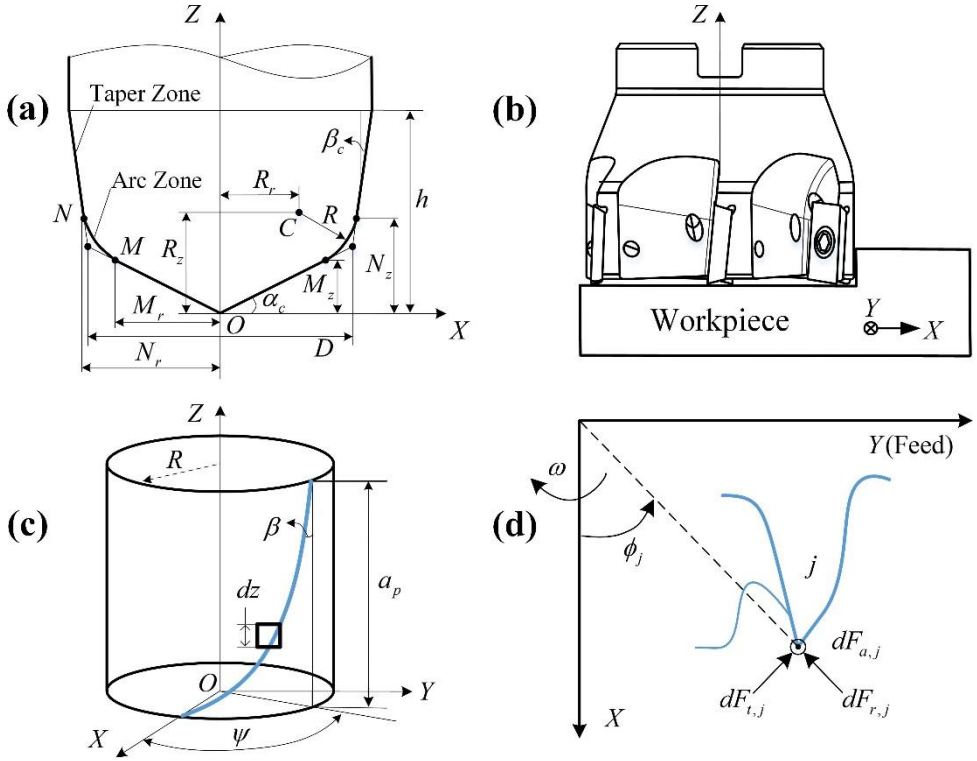

Fig.1 Geometric model of the general end mill. (a) General end milling cutter. (b) Taper end milling cutter. (c) Cutting edge geometry of end mill. (d) Analysis of the force on the tooth.

2.2 Identification of milling force coefficients

According to the fast calibration method [34], the milling force coefficients can be calculated quickly and accurately. Assuming that the measured average milling force is equal to the nominal value of milling force, then the milling force coefficients can be expressed as:

$$\overline{F_x} = \frac{Na_p f_t}{8\pi}\left[K_{tc}(\cos 2\phi_{ex} - \cos 2\phi_{st}) - K_{rc}(2\phi_{ex} - 2\phi_{st} - (\sin 2\phi_{ex} - \sin 2\phi_{st}))\right] + \frac{Na_p}{2\pi}\left[-K_{\text{te}}(\sin 2\phi_{ex} - \sin 2\phi_{st}) + K_{re}(\cos\phi_{ex} - \cos\phi_{st})\right]$$

$$\overline{F_y} = \frac{Na_p f_t}{8\pi}\left[K_{rc}(\cos 2\phi_{ex} - \cos 2\phi_{st}) + K_{tc}(2\phi_{ex} - 2\phi_{st} - (\sin 2\phi_{ex} - \sin 2\phi_{st}))\right] - \frac{Na_p}{2\pi}\left[K_{re}(\sin 2\phi_{ex} - \sin 2\phi_{st}) + K_{te}(\cos\phi_{ex} - \cos\phi_{st})\right] \quad (4)$$

$$\overline{F_z} = \frac{Na_p}{2\pi}\left[K_{ae}(\phi_{ex} - \phi_{st}) - K_{ac} f_t(\cos\phi_{ex} - \cos\phi_{st})\right]$$

where $\overline{F_x}$, $\overline{F_y}$, and $\overline{F_z}$ are the average forces over a tooth period, a_p is the axial cutting width, and ϕ_{st}, ϕ_{ex} are the tooth angle of entrance and exit respectively. When the machining type is down milling, $\phi_{st} = \pi - \arccos(1 - a_e / R)$, and $\phi_{ex} = \pi$, where a_e is the radial cutting width and R is the tool radius. The matrices of the average forces and force coefficients can be shown in Eq.(5)：

$$\begin{bmatrix} \overline{F_{x1}} \\ \overline{F_{y1}} \\ \overline{F_{z1}} \\ \overline{F_{x2}} \\ \overline{F_{y2}} \\ \overline{F_{z2}} \\ \text{M} \end{bmatrix} = \begin{bmatrix} A_{1x_1} & A_{2x_1} & A_{3x_1} & A_{4x_1} & 0 & 0 \\ A_{1y_1} & A_{2y_1} & A_{3y_1} & A_{4y_1} & 0 & 0 \\ 0 & 0 & 0 & 0 & A_{5z_1} & A_{6z_1} \\ A_{1x_2} & A_{2x_2} & A_{3x_2} & A_{4x_2} & 0 & 0 \\ A_{1y_2} & A_{2y_2} & A_{3y_2} & A_{4y_2} & 0 & 0 \\ 0 & 0 & 0 & 0 & A_{5z_2} & A_{6z_2} \\ \text{M} & \text{M} & \text{M} & \text{M} & \text{M} & \text{M} \end{bmatrix} \cdot \begin{bmatrix} K_{tc} \\ K_{te} \\ K_{rc} \\ K_{re} \\ K_{ac} \\ K_{ae} \end{bmatrix} \quad (5)$$

Matrix $[\mathbf{A}]$ is related to milling parameters, and its elements can be expressed as:

$$
\begin{aligned}
A_{1x_i} &= \frac{Na_p f_t}{8\pi}(\cos 2\phi_{ex} - \cos 2\phi_{st}) \\
A_{2x_i} &= \frac{Na_p}{2\pi}(\sin \phi_{st} - \sin \phi_{ex}) \\
A_{3x_i} &= \frac{Na_p f_t}{8\pi}(2\phi_{st} - 2\phi_{ex} + (\sin 2\phi_{ex} - \sin 2\phi_{st})) \\
A_{4x_i} &= \frac{Na_p}{2\pi}(\cos \phi_{ex} - \cos \phi_{st}) \\
A_{1y_i} &= \frac{Na_p f_t}{8\pi}(2\phi_{ex} - 2\phi_{st} - (\sin 2\phi_{ex} - \sin 2\phi_{st})) \\
A_{2y_i} &= \frac{Na_p}{2\pi}(\cos \phi_{st} - \cos \phi_{ex}) \\
A_{3y_i} &= \frac{Na_p f_t}{8\pi}(\cos 2\phi_{ex} - \cos 2\phi_{st}) \\
A_{4y_i} &= \frac{Na_p}{2\pi}(\cos \phi_{st} - \cos \phi_{ex}) \\
A_{5z_i} &= \frac{Na_p f_t}{2\pi}(\cos \phi_{st} - \cos \phi_{ex}) \\
A_{6z_i} &= \frac{Na_p}{2\pi}(\phi_{ex} - \phi_{st})
\end{aligned}
\tag{6}
$$

Finally, least square estimation can be used in Eq.(5) to calculate the cutting force coefficients, as shown in Eq.(7)：

$$
[\mathbf{K}] = (\mathbf{A}^{\mathrm{T}}\mathbf{A})^{-1}\mathbf{A}^{\mathrm{T}}\mathbf{F} \tag{7}
$$

The following section verifies the milling force coefficients as calculated in Eq. (7).

3. Verification of milling force coefficients by experiment

3.1 Experimental setup

A series of tests were conducted on a three-axis milling machine to verify the milling force coefficients during monitoring. The instantaneous milling forces were measured by a dynamometer (model: Kistler 9265B), as shown in Fig. 2(a). The sampling frequency was set to 2 kHz. Titanium alloy (model: Ti-6Al-4V) was chosen as the workpiece with a size of 180mm*140mm*90mm, and two teeth cemented

carbide cutter with a diameter of 50mm was used.

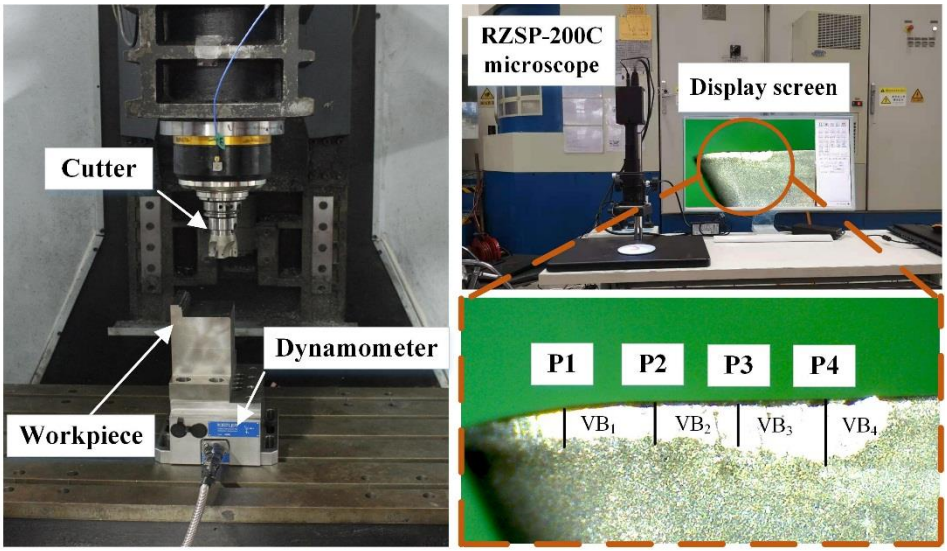

(a) Experiment system (b) Tool wear measurement

Fig. 2 Experiment setup and tool wear measurement

A stereo microscope (model: RZSP-200C) with an accuracy of 0.01mm was used to measure the area of wear on the tool flank (value VB) after a certain milling time, as shown in Fig. 2 (b). The experiment was stopped when one of the cutting edges' maximum value of VB reached 0.5mm. The milling parameters used in the tests are listed in Table 1, and down milling was adopted without fluid in X direction. A total of 10 tests were designed, the first seven tests with fixed parameters, and the last three tests with variable milling parameters, as shown in Fig. 3.

Table 1 The milling parameters in experiments

Test	Spindle speed (rpm)	Feed Rate (F) (mm/min)	a_p (mm)	a_e (mm)
1	600	48	2	4
2	1000	140	3	2
3	1200	120	2	2
4	1200	120	2	5
5	1500	180	2	2
6	1500	150	2	3
7	1500	75	2	4
8	900	108~180	2.5	1~5
9	600	120~180	3	1~4
10	1200	192~288	2	1~3

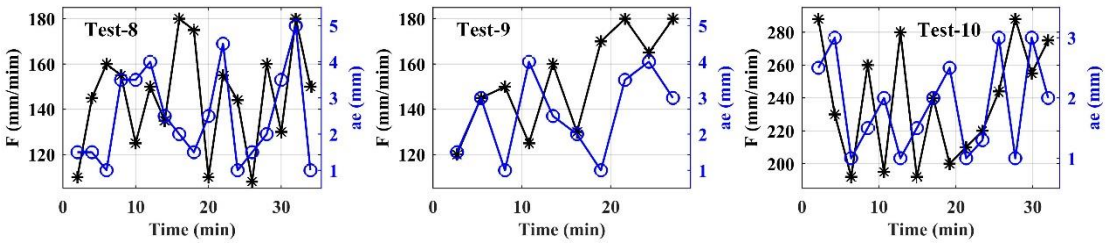

Fig. 3 The milling parameters in details.

When tool wear occurs, the contact between the cutter and the workpiece changes from one dimensional (a line) to two dimensional (a surface), leading to an increase in the milling force. However, the tool wear area on the flank is typically irregular, as shown in Fig. 4. The value of VB was measured four times and the mean value was calculated as follows:

$$\overline{VB} = \frac{\sum_{i=1}^{N} VB_i}{N} \quad (N = 4) \tag{8}$$

where VB_i is the measured value at equal intervals, as shown in Fig. 2 (b), and the wear areas on the tool flank is expressed as:

$$WearArea = \overline{VB} \cdot a_p \tag{9}$$

Tool wear progression is illustrated in Fig. 5 according to the calculation in Eq. (9). The tool flank wear behaves differently in each milling test. The reason for this may be related to the varying milling parameters applied and random behavior of tool wear. It can be seen from Fig.4 that in severe wear, the geometry of the tool changes, and there is slight chipping.

The International Standard Organization (ISO) has defined the failure criteria for tool wear. However, in actual machining, the cutter transitions to the stage of severe wear before it reaches the failure criteria. In general, the tool needs to be replaced when it reaches the stage of severe wear, in order to prevent damage to the parts. Therefore, tool wear is divided into two states: normal wear (the initial wear is defined as the normal wear state) and severe wear (Fig. 5). The inflection point between the two states identifies the point of tool failure, at which point the tool needs to be replaced.

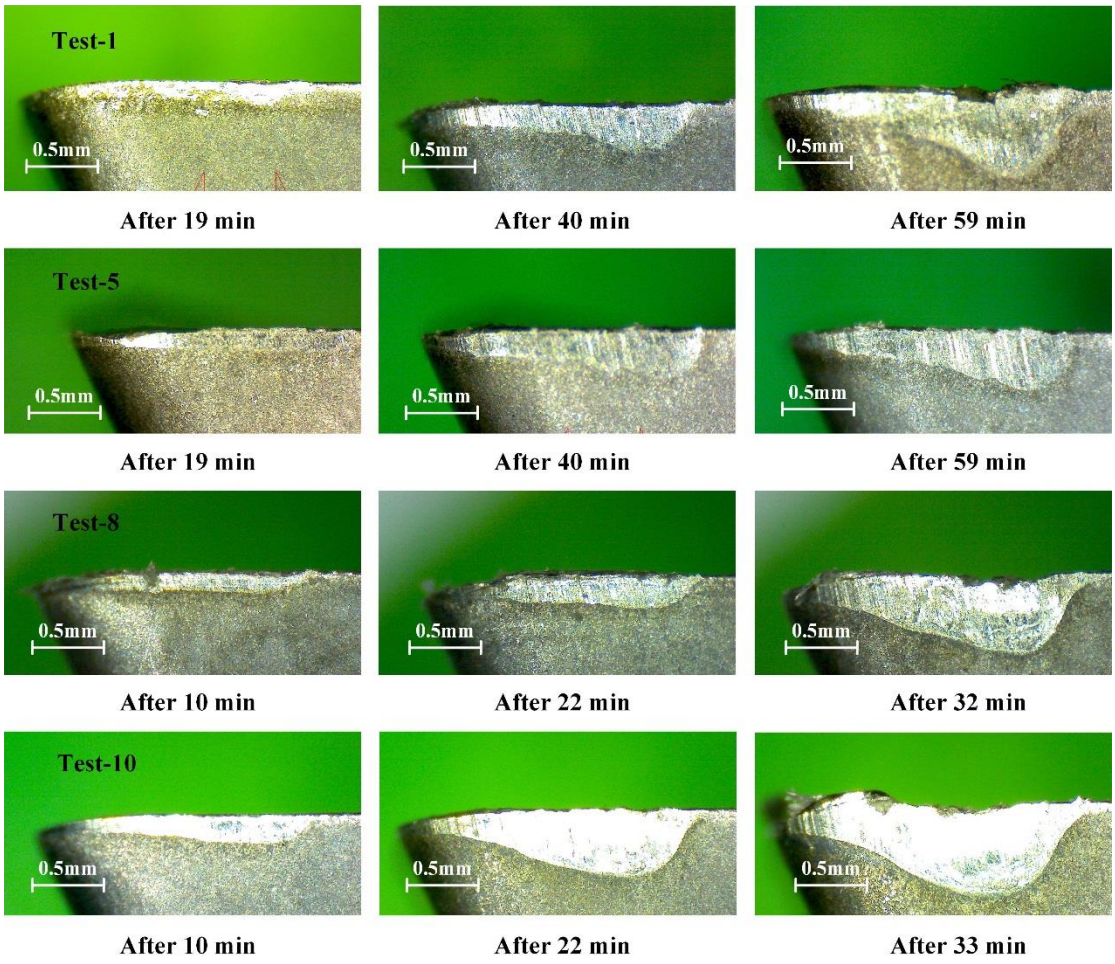

Fig. 4 Pictures of tool wear on the tool flank in different states of wear.

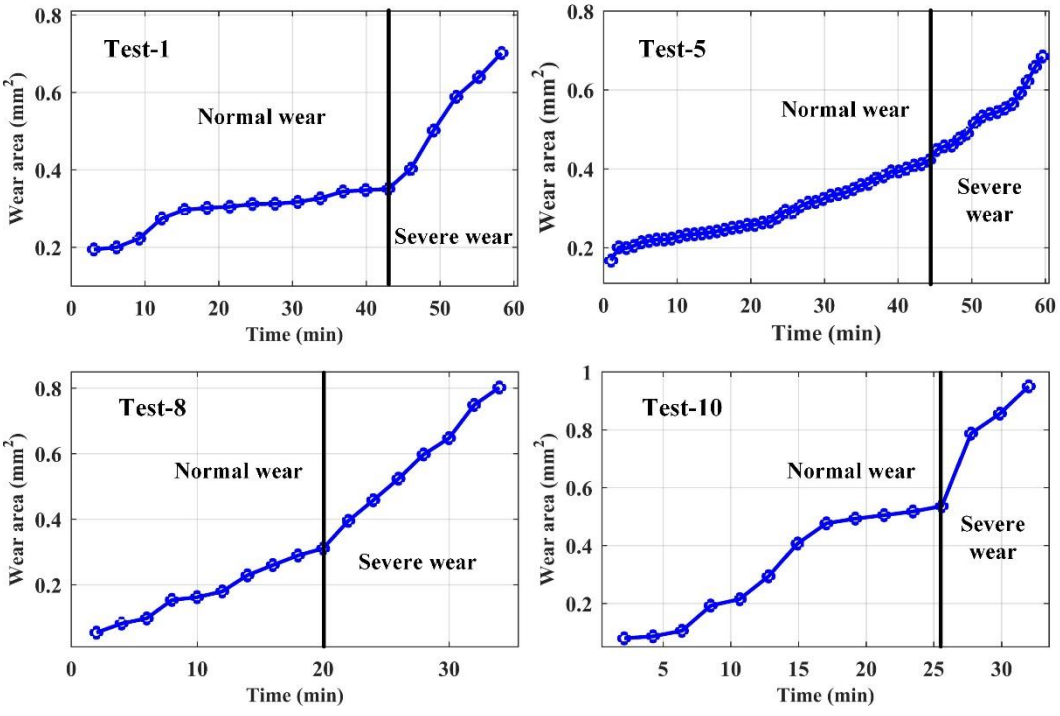

Fig. 5 The wear area on the tool flank.

3.2 Calculation of milling force coefficients

The coefficients of the cutting force and the edge force can be obtained from Eq. (5) to Eq. (7) by milling twice. Therefore, the sliding window method is used to calculate the coefficients [32]. Both the cutting force coefficients and edge force coefficients can reflect the tool wear, and are the best indexes for monitoring tool wear.

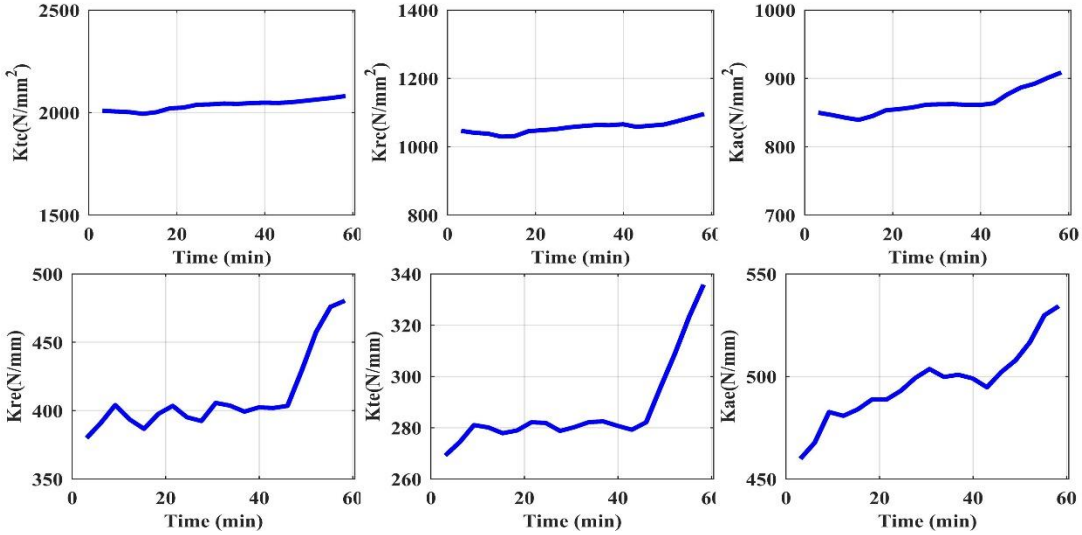

Fig. 6 Variable trend of milling force coefficient with milling time in Test-1.

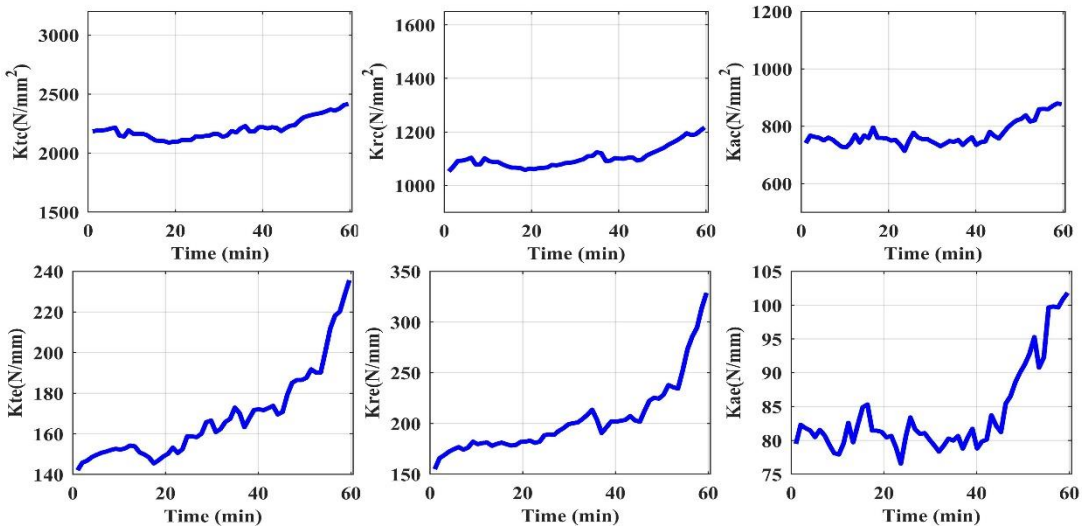

Fig. 7 Variable trend of milling force coefficient with milling time in Test-5.

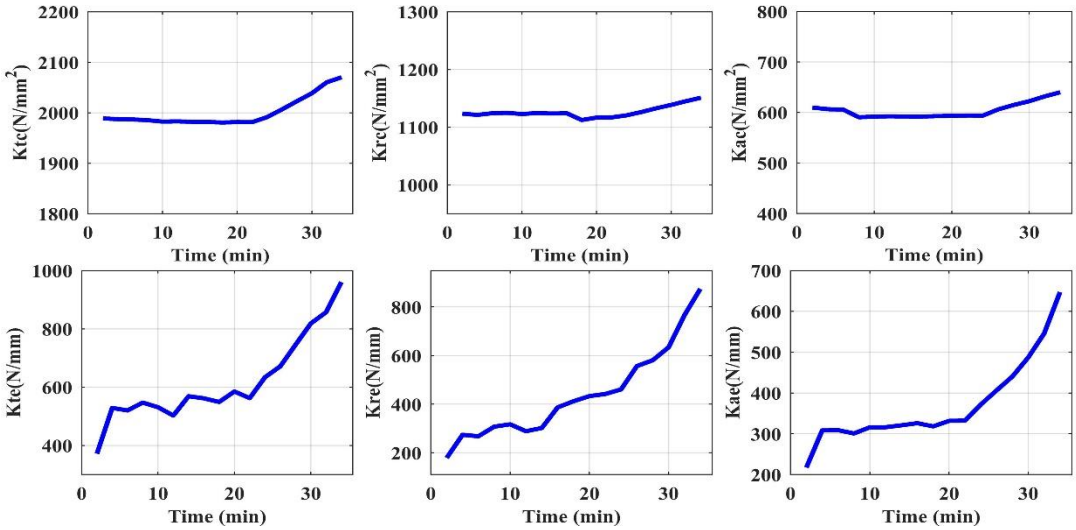

Fig. 8 Variable trend of milling force coefficient with milling time in Test-8.

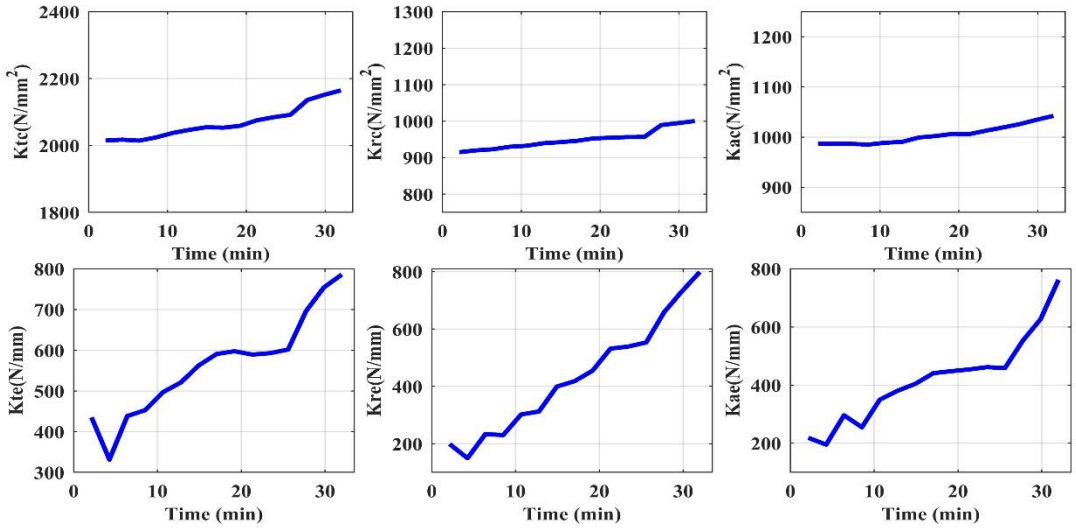

Fig. 9 Variable trend of milling force coefficient with milling time in Test-10

Fig. 6~9 show the variable trends of the milling force coefficients with milling time. It seems that the change of cutting force coefficients (*Ktc*, *Krc*, *Kac*) changes stability, with only an upward trend in the state of severe wear. The cutting force coefficient is only related to the geometric dimensions of the tool. With progressive tool wear, the shape of the tool changes (edge, fillet, etc.), leading to variation of the cutting force coefficients. On the contrary, the edge force coefficients (*Kte*, *Kre*, *Kae*) are related to tool wear, and their variations are caused by tool wear, which is not affected by milling parameters. The validity of six coefficients reflecting tool wear state is different. In addition, random factors in the milling process (vibration, chip entrapment, and so on), will affect the value of the coefficient. Moreover, the sensitivity of the coefficients in

different directions is also different. Therefore, it is necessary to fuse the six coefficients to reflect the state of tool wear. And the fused features are not sensitive to the milling parameters and have a strong correlation with tool wear.

4. Tool wear monitoring using milling force coefficients

4.1 Tool wear feature fusion via PCA method

The number of features should be as large as possible in order to accurately describe the tool wear state. However, previous research has found that not all extracted features are useful [7, 29]. Reducing features uncritically may cause the loss of a lot of information, resulting in wrong results because of the certain correlation among those features. Therefore, it is necessary to transform the original features into uncorrelated ones, and then fewer features can be used to represent the information.

The PCA algorithm maps features from dimensions n to k ($k < n$)by finding a set of orthonormal bases, which achieve the purpose of fusion. In order to find the orthogonal basis $\mathbf{u} = \{\mathbf{u}_1, \mathbf{u}_2, ...\mathbf{u}_k\}$, the variance of the fused sample features can be expressed as:

$$\frac{1}{m}\sum_{i=1}^{m}(\mathbf{x}^{(i)^{\mathrm{T}}}\mathbf{u})^2 = \frac{1}{m}\sum_{i=1}^{m}\mathbf{u}^{\mathrm{T}}\mathbf{x}^{(i)}\mathbf{x}^{(i)^{\mathrm{T}}}\mathbf{u} \tag{10}$$

where m is the number of samples and $\mathbf{x}$ is the matrix of sample features, whose dimension is n. Denote $\frac{1}{m}\sum_{i=1}^{m}(\mathbf{x}^{(i)^{\mathrm{T}}}\mathbf{u})^2$ as $\boldsymbol{\lambda}$, $\frac{1}{m}\sum_{i=1}^{m}\mathbf{x}^{(i)}\mathbf{x}^{(i)^{\mathrm{T}}}$ as $\boldsymbol{\Lambda}$. Eq.(10) can be rewritten as:

$$\boldsymbol{\lambda} = \mathbf{u}^{\mathrm{T}}\boldsymbol{\Lambda}\mathbf{u} \tag{11}$$

where $\boldsymbol{\lambda}$ is the eigenvalue of $\boldsymbol{\Lambda}$, and $\mathbf{u}$ is the eigenvector. Therefore, the best orthogonal basis is the eigenvector corresponding to the maximum eigenvalue. Eigenvalue decomposition of matrix $\boldsymbol{\Lambda}$ and the eigenvectors corresponding to the first k eigenvalues were selected. Therefore, the fused features can be expressed as:

$$\mathbf{Y}_{m\times k} = \mathbf{x}_{m\times n} \cdot \mathbf{u}_{n\times k} \tag{12}$$

The specific process is shown in Fig.10. And the milling force coefficients are obtained from milling forces used through Eq. (4) to Eq. (7).

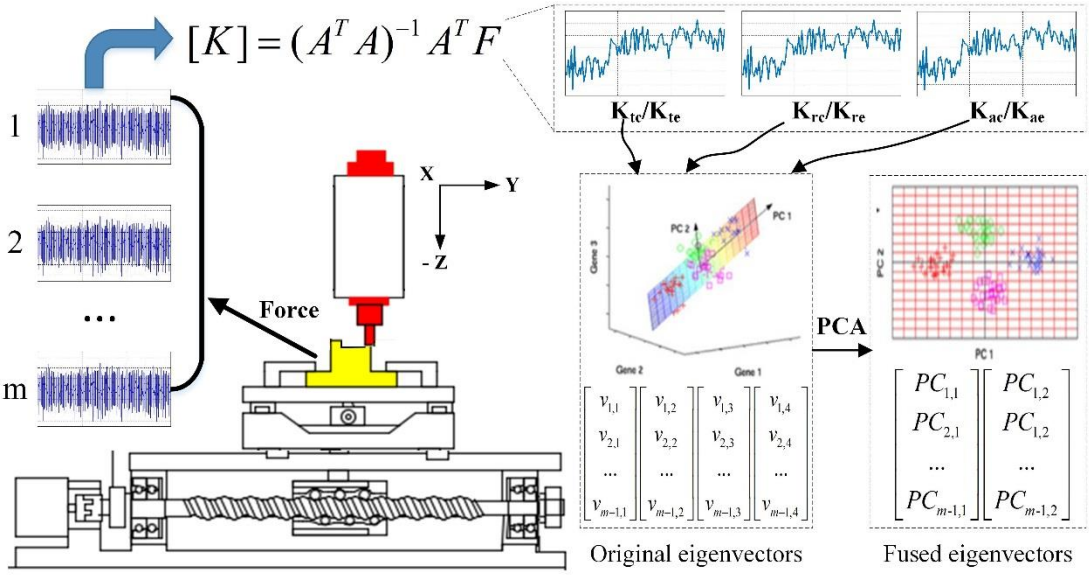

Fig. 10 Schematic diagram of features extraction and fusion of milling force coefficients.

In order to eliminate the influence of dimension, the 0-means method is used to normalize the milling force coefficients. The normalized results were used as input in the PCA algorithm to obtain the fused feature vector. The weight proportion of eigenvalue was set as > 95%. The fused features are shown in Fig.11. The PCA method integrates six-dimensional tool wear features into two dimensions, the results of which can distinguish tool states distinctly. According to the performance of the fused features and the actual application requirements, the tool wear can be monitored by the SVM algorithm.

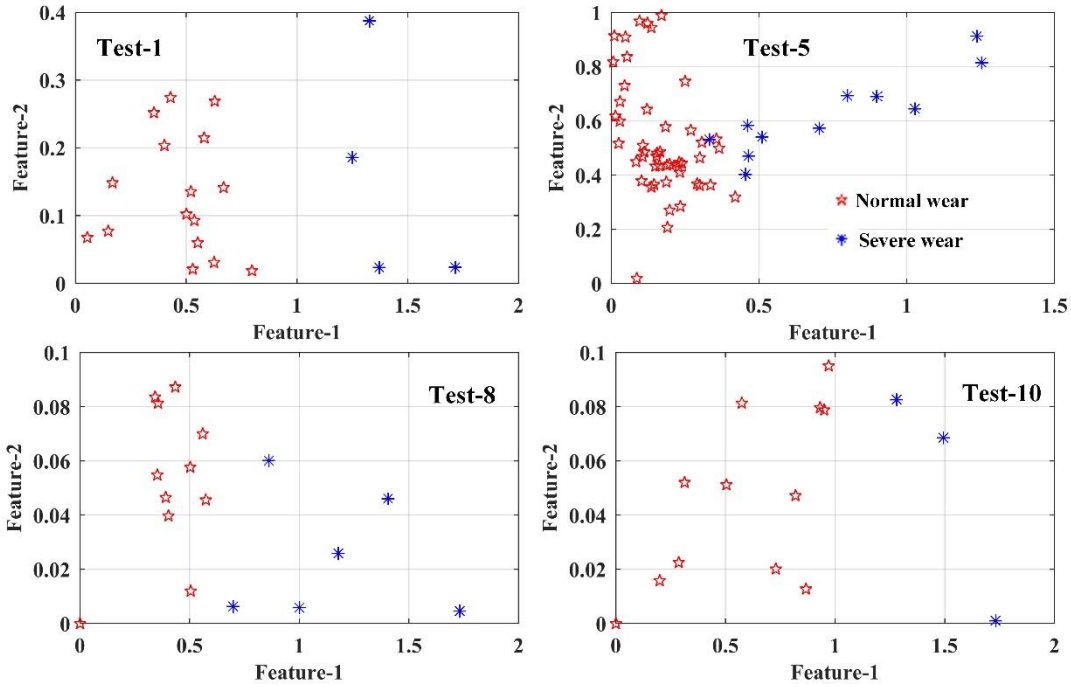

Fig. 11 The fused features using PCA.

4.2 The monitoring of tool wear state via c-SVM method

Taking the fused feature of Test-1 as an example, as show in Fig. 12, a hyperplane is found in the fused feature sample space to separate different tool states, which can be shown as:

$$y = \boldsymbol{\omega}^{\mathrm{T}}\mathbf{x} + b = 0 \tag{13}$$

where $\boldsymbol{\omega}$ is the normal vector determining the direction of the hyperplane, and b is the displacement term expressing the distance between the hyperplane and the origin. The nearest training sample points to the hyperplane are called support vectors. The sum of the distances between the two heterogeneous support vectors and the hyperplane is called the margin, expressed as γ. Therefore, the core of using a support vector machine to monitor the tool wear state is to find the optimal hyperplane; that is, to satisfy the parameters $\boldsymbol{\omega}$ and b constrained in Eq.(13)to maximize the value of γ.

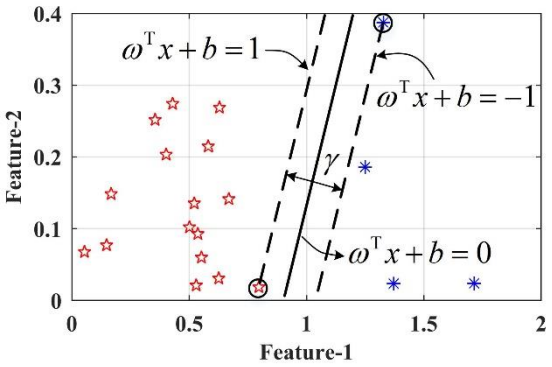

Fig.12 The diagram of tool wear monitoring using c-SVM.

Suppose the training data and its label are $\left\{x^{(i)}, y^{(i)}\right\} i=1,2,3...m$， $y^{(i)} \in \{0,2\}$. The c-SVM of the L1 regular soft boundary can be expressed as:

$$\begin{aligned} &\min_{\omega,b} \frac{1}{2}\|\boldsymbol{\omega}\|^2 + C\sum_{i}^{m}\xi_i \\ &s.t. \quad y^{(i)}(\boldsymbol{\omega}^{\mathrm{T}}\mathbf{x}^{(i)}+b) \geq 1-\xi_i, \xi_i \geq 0 \end{aligned} \tag{14}$$

where C is the regularization parameter and ξ is the relaxation factor. According to the optimization theory [35], the dual problem is shown as follows:

$$\begin{aligned} &\min \frac{1}{2}\sum_{j=1}^{m}\sum_{i=1}^{m}\alpha_i Q_{ij}\alpha_j - \sum_{i}^{m}\alpha_i \\ &s.t. \quad \sum_{i}^{m} y^{(i)}\alpha_i = 0, 0 \leq \alpha_i \leq C \end{aligned} \tag{15}$$

where α_i is a Lagrange polynomial. $Q_{ij} = y^{(i)}y^{(j)}K(\mathbf{x}^{(i)}, \mathbf{x}^{(j)})$, K is a kernel function. The quadratic programming (QP) problem in Eq.(15)is generally solved by sequential minimal optimization (SMO). The optimal solutions are $\left\{\alpha_i^*, b^*\right\} i=1,2,3...m$.

For a new sample $\mathbf{x}^{(c)}$, the discriminant function is given by:

$$\begin{aligned} &f(\mathbf{x}^{(c)}) = \boldsymbol{\omega}^{\mathrm{T}}\mathbf{x}^{(c)} + b^* = \sum_{j=1}^{m}\alpha_j^* y^{(j)}K(\mathbf{x}^{(c)}, \mathbf{x}^{(j)}) + b^* \\ &if \ \ f(\mathbf{x}^{(c)}) \geq 0, then \ y^{(c)} = 1; f(x^{(c)}) < 0, then \ y^{(c)} = -1 \end{aligned} \tag{16}$$

Therefore, ten groups of data set allocations are shown in Table 2 (277 samples in total), nine of which are used as a training set and one as a testing set in turn (cross-validation). The input of the c-SVM model is the fused features of milling force coefficients, and the output is the tool state (normal wear is 0, severe wear is 2). The

model parameters C = 10, and scale = 1 (Gaussian kernel coefficient) are set. The modeled results are compared with the measured results, as shown in Fig. 13.

Table 2 Tool wear state classification

Tool states	Number of samples	Labels
Normal wear	205	0
Severe wear	72	2

Fig. 13 shows that the milling force coefficient can be used to monitor tool wear status, especially for variable milling parameters. The reason is that the milling force coefficient eliminates the influence of milling parameters and relates to the tool state directly. Besides, the alternating stress of the tool changes greatly with variable milling parameters, thus the tool wear ratio is fast. However, the error in Test-5 is bigger because the milling force coefficient shows that the tool has transited the severe stage at 40 min or earlier as shown in Fig.7. But Fig.5 shows that the actual measured value of the wear area transitions to the severe stage at 45min.The reason for this is that the vibration in the milling process has a great influence on the milling force, and the milling force coefficients cannot reflect the tool wear state well.

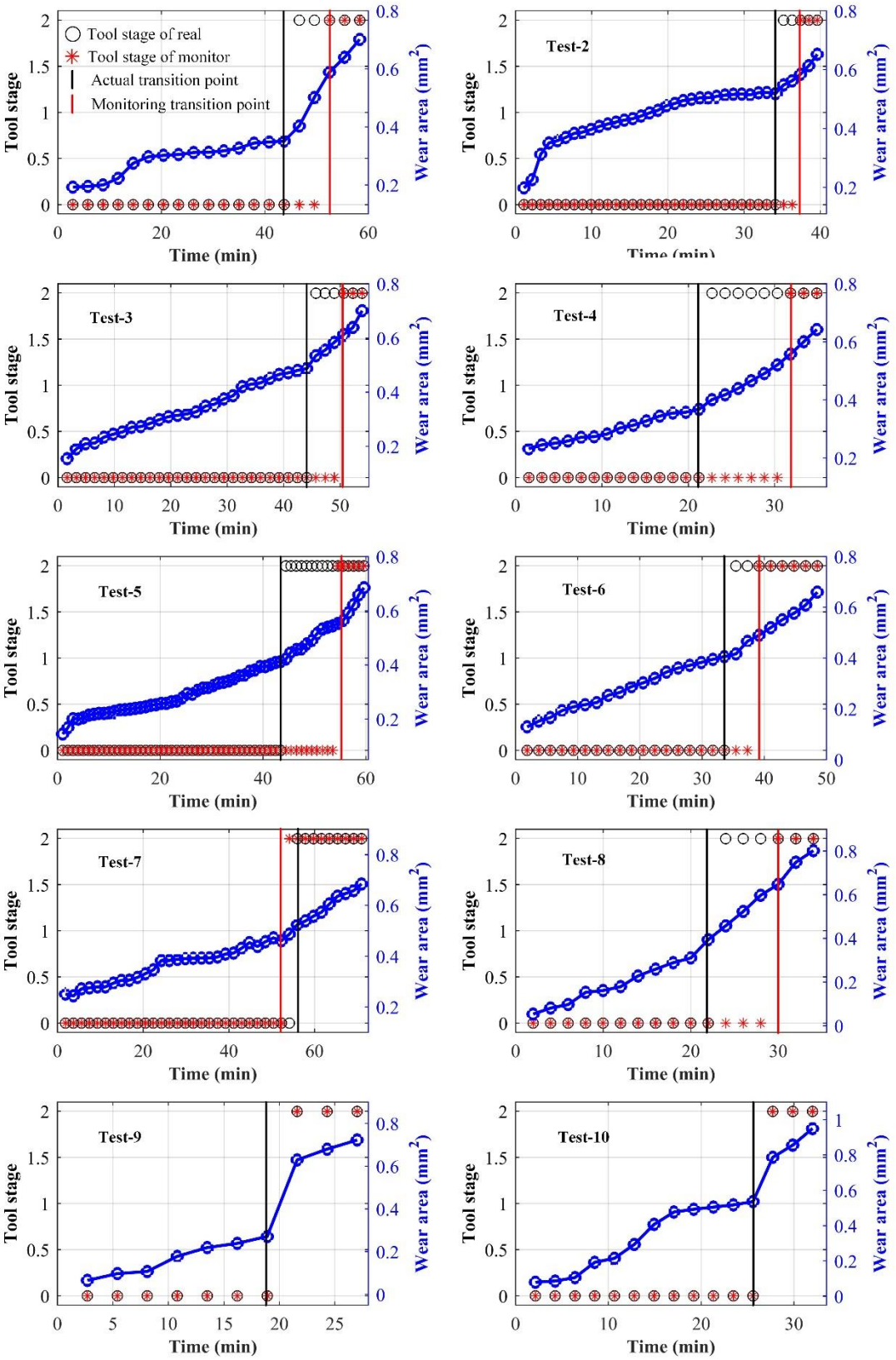

Fig. 13 The detection results of tool wear state.

4.3 The comparison with traditional tool wear features

In general, the traditional tool wear features are divided into three types: time domain, frequency domain, and time-frequency domain [29]. According to the literature [7, 8], RMS, kurtosis, and the wavelet packets energy spectrum can be extracted from the time and time-frequency domain respectively. Due to the fact that the milling force can be resolved into three directions of x, y, and z, there are 30 features.

According to the method described in Section 4.1, the extracted features can be fused into three dimensions. Then the fused features form the input of the c-SVM model in section 4.2 (the model parameters are unchanged), and the results are shown in Fig.14.

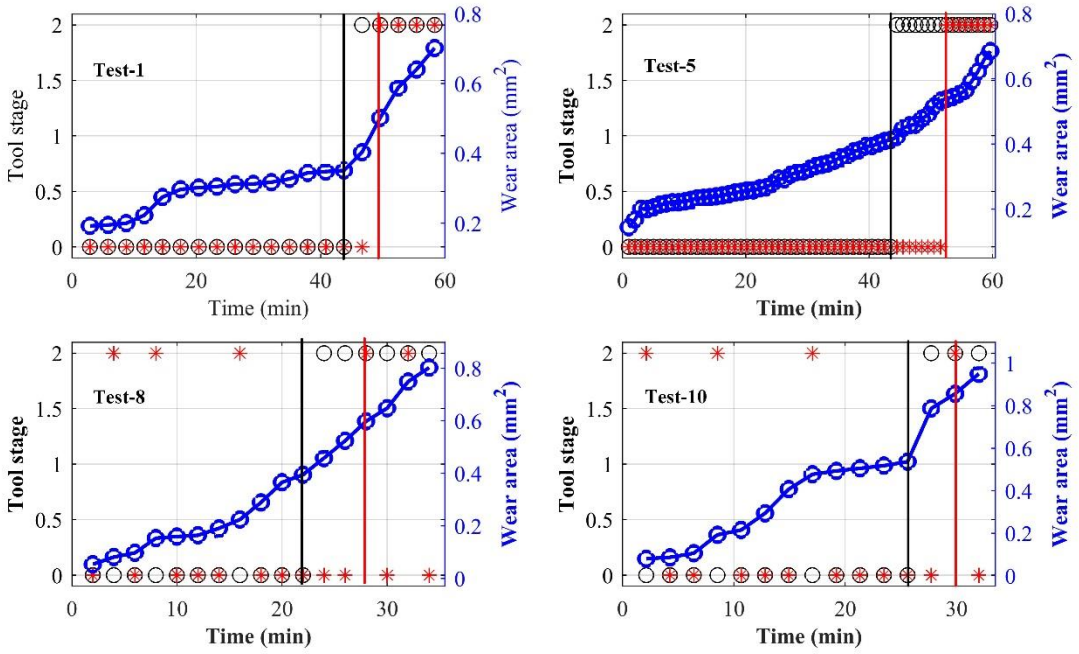

Fig.14 The detection results of tool wear state using traditional features.

The general evaluation index is expressed as:

$$accuracy = T \big/ (T + F) \tag{17}$$

where T is the number of correctly monitoring samples, and F is the number of incorrectly monitoring samples. Assuming that the results are all normal wear, the accuracy is 74% which is not suitable. Using a confusion matrix can solve the problem of data imbalance [36]. Table 3 lists a comparison of monitoring accuracy between traditional features and milling force coefficients. The larger the true positive rate (TPR)

and the smaller the false positive rate (FPR), the more reasonable is the feature. For the convenience of comparison, the indicators can be expressed as follows:

$$Index = \overline{TPR} \Big/ \overline{FPR} \tag{18}$$

According to Eq.(18), the indexes are 2.15 and 2.75 by using traditional features and milling force coefficients, respectively. The results show that the accuracy of tool wear monitoring using milling force coefficients can be improved by nearly 30% compared with the existing traditional features.

Table 3 Comparison of the accuracy between the proposed features and the general features (%)

Test	Force coefficients		Traditional features	
	TPR	FPR	TPR	FPR
1	1	0.4	1	0.2
2	1	0.4	1	0.4
3	1	0.5	1	0.17
4	1	0.67	1	0.56
5	1	0.69	1	0.63
6	1	0.29	1	0.29
7	0.97	0	1	0
8	1	0.67	0.73	0.67
9	1	0	0.67	0.67
10	1	0	0.75	0.67
Average	0.997	0.362	0.915	0.426

In addition, Table 3 shows that under the fixed milling parameters, the monitoring accuracy of traditional features is higher than that of milling force coefficients. Because the traditional feature represents the tool wear from different dimensions (time domain, frequency domain, time-frequency domain), thus the monitoring accuracy is higher. However, there are many differences in monitoring accuracy under variable parameters. Due to the traditional features are difficult to distinguish whether the forces change is caused by tool wear or the variable of milling parameters. As shown in Fig.15, taking RMS as an example, the trend of the RMS data follows the milling forces, and cannot reflect the trend of tool wear (Fig.15 (d-f)) due to the influence of milling parameters. However, the milling force coefficients are not affected by milling parameters (Fig.15 (g-i)), which reflect the wear trend of the tool. Therefore, the milling force coefficient can be used to monitor the tool wear under variable milling parameters. In addition, as

shown in Fig.14, the traditional features are frequently misjudged under variable milling parameters, and cannot be used during the actual machining process.

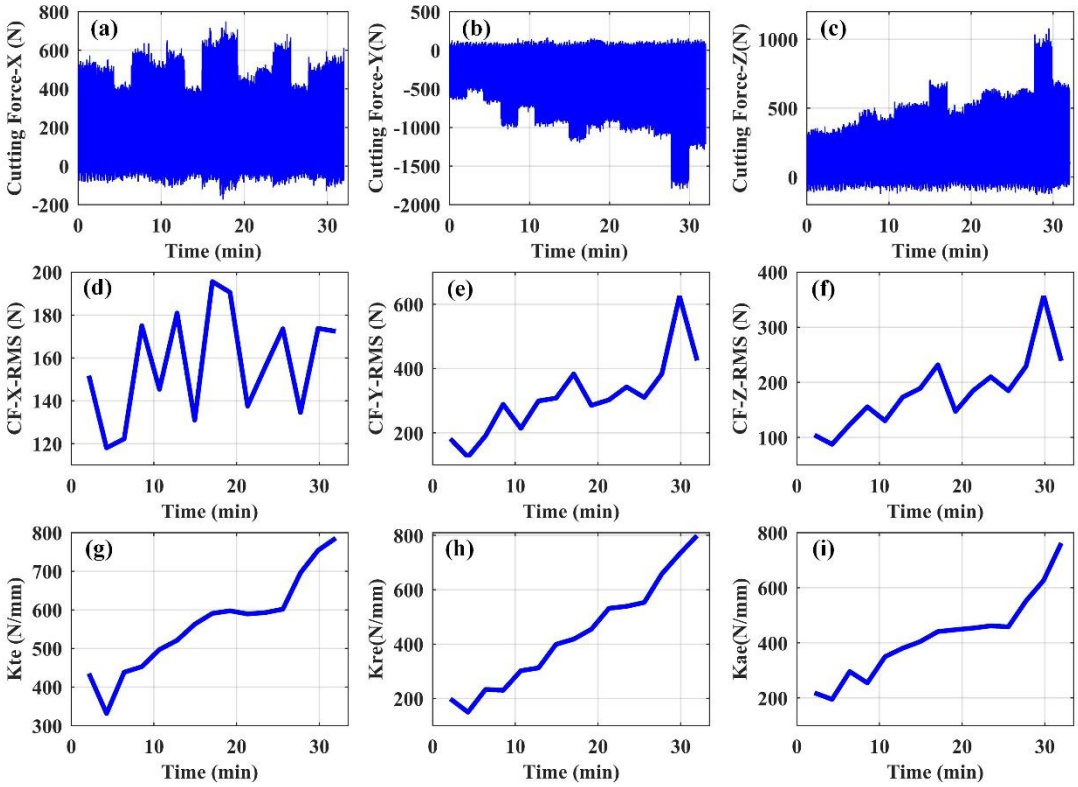

Fig. 15 Comparison of RMS feature and milling force coefficient feature in the parameters of Test-5.

5. Conclusions

A tool wear monitoring method based on feature extraction and fusion from milling forces is proposed. The transition point from normal wear to severe wear (tool failure) is used to judge whether the tool is invalid. Many milling experiments were conducted using a cemented carbide blade and a titanium alloy (TC4) workpiece under different milling parameters. The conclusions are as follows:

1. Compared with the traditional features present when using fixed milling parameters, the milling force coefficients calculated based on the instantaneous milling force model can well reflect the trend of tool wear under variable milling parameters.

2. Due to the differing correlations of cutting force coefficients and edge force coefficients to tool wear, the feature fused by PCA can accurately reflect the tool wear

state with fewer features.

3. The c-SVM algorithm was selected as the tool wear monitoring model, and the fused features of milling force coefficients were used as the input. The results show that the accuracy of tool wear monitoring can be improved by 30% compared with the traditional features used for tool wear monitoring, which has significant advantages in tool wear monitoring when using variable milling parameters.

Declarations

Consent to publish: The authors consent that the work entitled as "Milling force coefficients-based tool wear monitoring for variable parameters milling" for possible publication in International Journal of Advanced Manufacturing Technology. The authors claim that the research in this paper is the authors' original work and has not been published nor has it been submitted simultaneously elsewhere.

Author's contributions: Tianhang Pan: Methodology, Data curation, Experiment, Validation, Formal analysis, Writing – original draft, review & editing; **Jun Zhang:** Supervision, Writing – review & editing; **Xing Zhang:** Methodology, Formal analysis, Writing – review & editing; **Wanhua Zhao**: Methodology, Supervision, Data curation, Formal analysis; **Huijie Zhang:** Experiment; **Bingheng Lu**: Project administration.

Funding: This work was financially supported by the National Key R&D Program of China (No. 2018YFB1701901) for Jun Zhang, the Key-Area R&D Program of Guangdong Province (No. 2020B090927002) for Huijie Zhang, the National Key R&D Program of China (No. 2018YFB1701901), the Major Science and Technology Project of Shaanxi Province (No. 2019zdzx01-01-02), and the China Postdoctoral Science Foundation (No. BX20180253, 219945) for Xing Zhang.

Competing interests: The authors declare that they have no known competing financial interests or personal relationships that could have appeared to influence the work reported in this paper.

Availability of data and materials: All data generated or analyzed during this study

are included in this article.

References

[1] Duro JA, Padget JA, Bowen CR, Kim HA, Nassehi A. Multi-sensor data fusion framework for cnc machining monitoring. Mechanical Systems & Signal Processing 2016;66–67:505-520. https://doi.org/10.1016/j.ymssp.2015.04.019

[2] Tobon-Mejia DA, Medjaher K, Zerhouni N. CNC machine tool's wear diagnostic and prognostic by using dynamic Bayesian networks. Mechanical Systems & Signal Processing 2012;28-4:167–182. https://doi.org/10.1016/j.ymssp.2011.10.018

[3] Mohanraj T, Shankar S, Rajasekar R, Sakthivel NR, Pramanik A. Tool condition monitoring techniques in milling process-a review. Journal of Materials Research and Technology 2020;9(1):1032–1042. https://doi.org/10.1016/j.jmrt.2019.10.031

[4] D'Addona AMM, Ullah AMMS, Matarazzo D. Tool-wear prediction and pattern-recognition using artificial neural network and DNA-based computing. Journal of Intelligent Manufacturing 2017; 28:1285–1301. https://doi.org/10.1007/s10845-015-1155-0

[5] Elgargni M, Al-Habaibeh A, Lotfi A. Cutting tool tracking and recognition based on infrared and visual imaging systems using principal component analysis (PCA) and discrete wavelet transform (DWT) combined with neural networks. The International Journal of Advanced Manufacturing Technology 2015; 77:1965–1978. https://doi.org/10.1007/s00170-014-6576-y

[6] Amzi AI. Monitoring of tool wear using measured machining forces and neuro-fuzzy modeling approaches during machining of GFRP composites. Advances in Engineering Software 2015; 82:53-64. https://doi.org/10.1016/j.advengsoft.2014.12.010

[7] Li N, Chen YJ, Kong DD, Tan SL. Force-based tool condition monitoring for turning process using v-support vector regression. The International Journal of Advanced Manufacturing Technology 2017;91:351–361. https://doi.org/10.1007/s00170-016-9735-5

[8] Huang SN, Tan KK, Wong YS, Silva C, Goh HL, Tan W. Tool wear detection and fault diagnosis based on cutting force monitoring. International Journal of Machine Tools & Manufacture 2007; 47:444–451. https://doi.org/10.1016/j.ijmachtools.2006.06.011

[9] Anicic O, Jovic S, Stanojevic N, Marsenic M, Pejovic B, Nedic B. Estimation of tool wear according to cutting forces during machining procedure. Sensor Review 2018;38(2):176-180. https://doi.org/10.1108/SR-07-2017-0147

[10] Lee DE, Hwang I, Valente CMO, Oliveira JFG, Dornfeld DA. Precision manufacturing process monitoring with acoustic emission. International Journal of Machine Tools & Manufacture 2006; 46:176–188. https://doi.org/10.1016/j.ijmachtools.2005.04.001

[11] Kannatey-Asibu E, Yum J, Kim TH. Monitoring tool wear using classifier fusion. Mechanical Systems & Signal Processing. 2017; 85:651–661. https://doi.org/10.1016/j.ymssp.2016.08.035

[12] Bhuiyan MSH, Choudhury IA, Dahari M, Nukman Y, Dawal SZ. Application of acoustic emission sensor to investigate the frequency of tool wear and plastic deformation in tool condition monitoring. Measurement 2016; 92:208–217. https://doi.org/10.1016/j.measurement.2016.06.006

[13] Pechenin V, Khaimovich A, Kondratiev A, Bolotov M. Method of controlling cutting tool wear based on signal analysis of acoustic emission for milling. Procedia Eng 2017; 176:246–252.

https://doi.org/10.1016/j.proeng.2017.02.294
[14] Brili N , Ficko M , Klannik S. Automatic Identification of Tool Wear Based on Thermography and a Convolutional Neural Network during the Turning Process. Sensors 2021; 21:1917. https://doi.org/10.3390/s21051917
[15] Wang GF, Yang YW, Zhang YC, Xie QL. Vibration sensor based tool condition monitoring using v support vector machine and locality preserving projection. Sensors and Actuators A 2014; 209:24–32. https://doi.org/10.1016/j.sna.2014.01.004
[16] Ratava J, Lohtander M, Varis. J Tool condition monitoring in interrupted cutting with acceleration sensors. Robotics and Computer–Integrated Manufacturing 2017; 47:70–75. https://doi.org/10.1016/j.rcim.2016.11.008
[17] Khajavi MN, Nasernia E, Rostaghi M. Milling tool wear diagnosis by feed motor current signal using an artificial neural network. Journal of Mechanical Science and Technology 2016; 30 (11):4869-4875. https://doi.org/10.1007/s12206-016-1005-9
[18] Koike R, Ohnishi K, Aoyama T. A sensorless approach for tool fracture detection in milling by integrating multi-axial servo information. CIRP Annals - Manufacturing Technology 2016; 65:385-388. https://doi.org/10.1016/j.cirp.2016.04.101
[19] Silva LRRD, Frana PHP, Andrade CLF, Silva RBD, Guesser WL, Machado AR. Monitoring tool wear and surface roughness in the face milling process of high-strength compacted graphite cast irons. Journal of the Brazilian Society of Mechanical Sciences and Engineering 2021; 43:180. https://doi.org/10.1007/s40430-021-02897-7
[20] Zhu KP, Mei T, Ye DS. Online condition monitoring in micro milling: a force waveform shape analysis approach. IEEE Trans Ind Electron 2015; 62(6):3806–3813. https://doi.org/10.1109/TIE.2015.2392713
[21] Kim GD, Chu CN. Indirect cutting force measurement considering frictional behavior in a machining center using feed motor current. International Journal of Advanced Manufacturing Technology 1999; 15(7):478-484. https://doi.org/10.1007/s001700050092
[22] Caggiano A. Tool Wear Prediction in Ti-6Al-4V Machining through Multiple Sensor Monitoring and PCA Features Pattern Recognition. Sensors 2018; 18:823. https://doi.org/10.3390/s18030823
[23] Fang N, Pai P, Mosquea S. Effect of tool edge wear on the cutting forces and vibrations in high-speed finish machining of inconel 718: an experimental study and wavelet transform analysis. The International Journal of Advanced Manufacturing Technology 2011; 52:65–77. https://doi.org/10.1007/s00170-010-2703-6
[24] Zhou YQ, Sun BT, Sun WF. A tool condition monitoring method based on two-layer angle kernel extreme learning machine and binary differential evolution for milling. Measurement 2020; 166:180-186. https://doi.org/10.1016/j.measurement.2020.108186
[25] Liu T, Zhu KP, Wang G. Micro-milling tool wear monitoring under variable cutting parameters and runout using fast cutting force coefficient identification method. The International Journal of Advanced Manufacturing Technology 2020; 111:3175-3188. https://doi.org/10.1007/s00170-020-06272-z
[26] Stavropoulos P, Papacharalampopoulos A, Vasiliadis E, Chryssolouris G. Tool wear predictability estimation in milling based on multi-sensorial data. The International Journal of Advanced Manufacturing Technology 2016; 82:509-521. https://doi.org/10.1007/s00170-015-7317-6

[27] Xu XW, Tao ZR, Ming WW, An QL, Chen M. Intelligent monitoring and diagnostics using a novel integrated model based on deep learning and multi-sensor feature fusion. Measurement 2020; 165:108086. https://doi.org/10.1016/j.measurement.2020.108086
[28] Yao YX, Li XL, Yuan ZJ. Tool wear detection with fuzzy classification and wavelet fuzzy neural network. International Journal of Machine Tools and Manufacture 1999; 39(10):1525-1538. https://doi.org/10.1016/S0890-6955(99)00018-8
[29] Kong DD, Chen YJ, Li N, Tan SL. Tool wear monitoring based on kernel principal component analysis and v-support vector regression. International Journal of Advanced Manufacturing Technology 2017; 89:175–190. https://doi.org/10.1007/s00170-016-9070-x
[30] Wang JJ, Xie JY, Zhao R, Zhang LB, Duan LX. Multisensory fusion based virtual tool wear sensing for ubiquitous manufacturing. Robotics and Computer-Integrated Manufacturing 2016; 45(C):47-58. https://doi.org/10.1016/j.rcim.2016.05.010
[31] Zhu KP, Liu TS. On-line tool wear monitoring via hidden semi-Markov model with dependent durations. IEEE Transactions on Industrial Informatics 2018; 14-1:69-78. https://doi.org/10.1109/TII.2017.2723943
[32] Nouri M, Fussell BK, Ziniti BL, Linder E. Real-time tool wear monitoring in milling using a cutting condition independent method. International Journal of Machine Tools and Manufacture 2015; 89:1-13. https://doi.org/10.1016/j.ijmachtools.2014.10.011
[33] Engin S, Altintas Y. Mechanics and dynamics of general milling cutters. Part I: helical end mills. International Journal of Machine Tools and Manufacture 2001; 41:2195-2212. https://doi.org/10.1016/S0890-6955(01)00045-1
[34] Budak E, Altintas Y, Armarego EJA. Prediction of Milling Force Coefficients From Orthogonal Cutting Data. J*ournal of* Manufacturing Science and Engineering 1996; 118:216-224. https://doi.org/10.1115/1.2831014
[35] Xu GD, Chen JH, Zhou HC. A tool breakage monitoring method for end milling based on the indirect electric data of CNC system. The International Journal of Advanced Manufacturing Technology 2019; 101:419–434. https://doi.org/10.1007/s00170-018-2735-x
[36] Sun YM, Wong AKC, Kamel MS. Classification of imbalanced data: a review. International Journal of Pattern Recognition 2009; 23:687–719. https://doi.org/10.1142/s0218001409007326